University of Nebraska - Lincoln
DigitalCommons@University of Nebraska - Lincoln

Mechanical & Materials Engineering Faculty Publications

Mechanical & Materials Engineering, Department of

1-1-2007

Thermal characterization of microscale conductive and nonconductive wires using transient electrothermal technique

Jiaqi Guo
University of Nebraska - Lincoln

Xinwei Wang
University of Nebraska - Lincoln, xwang3@unl.edu

Tao Wang
State Key Laboratory of Clean Energy Utilization, Zhejiang University, Hangzhou, People's Republic of China

Follow this and additional works at: http://digitalcommons.unl.edu/mechengfacpub

Part of the Mechanical Engineering Commons

Guo, Jiaqi; Wang, Xinwei; and Wang, Tao, "Thermal characterization of microscale conductive and nonconductive wires using transient electrothermal technique" (2007). *Mechanical & Materials Engineering Faculty Publications.* Paper 8.
http://digitalcommons.unl.edu/mechengfacpub/8

This Article is brought to you for free and open access by the Mechanical & Materials Engineering, Department of at DigitalCommons@University of Nebraska - Lincoln. It has been accepted for inclusion in Mechanical & Materials Engineering Faculty Publications by an authorized administrator of DigitalCommons@University of Nebraska - Lincoln.

Thermal characterization of microscale conductive and nonconductive wires using transient electrothermal technique

Jiaqi Guo and Xinwei Wang[a)]
Department of Mechanical Engineering, N104 Walter Scott Engineering Center, University of Nebraska-Lincoln, Lincoln, Nebraska 68588-0656

Tao Wang
State Key Laboratory of Clean Energy Utilization, Zhejiang University, Hangzhou, People's Republic of China 310027

(Received 20 October 2006; accepted 24 January 2007; published online 28 March 2007)

In this paper, a transient technique is developed to characterize the thermophysical properties of one-dimensional conductive and nonconductive microscale wires. In this technique, the to-be-measured thin wire is suspended between two electrodes. When feeding a step dc to the sample, its temperature will increase and take a certain time to reach the steady state. This temperature evolution is probed by measuring the variation of voltage over the wire, which is directly related to resistance/temperature change. The temperature evolution history of the sample can be used to determine its thermal diffusivity. A 25.4 μm thick platinum wire is used as the reference sample to verify this technique. Sound agreement is obtained between the measured thermal diffusivity and the reference value. Applying this transient electrothermal technique, the thermal diffusivities of single-wall carbon nanotube bundles and polyester fibers are measured.
© *2007 American Institute of Physics*. [DOI: 10.1063/1.2714679]

I. INTRODUCTION

The thermophysical properties of carbon nanotubes (CNTs) prompted a wide variety of applications. Correspondingly, knowledge of thermal transport in these micro/nanoscale structures becomes considerably crucial to their engineering applications. To investigate the thermophysical properties of individual one-dimensional micro/nanostructures, limited experimental approaches have been developed. To date, the 3ω method,[1–4] microfabricated suspended device method,[5–7] and optical heating and electrical thermal sensing[8,9] (OHETS) technique are the leading measurement techniques to obtain thermophysical properties of wires/tubes at micro/nanoscales.

For the 3ω method, a sine/cosine current is fed to the sample, leading to its temperature variation at the second-harmonic frequency. As a result, the amplitude and phase shift of the third-harmonic voltage variation across the sample can be measured and used to characterize thermophysical properties. From the mechanism of the 3ω method, the sample is required to have linear *I-V* behavior within the applied ac voltage range. However, a large number of wires and tubes exhibit semiconductive properties. That is to say, they have the nonlinear *I-V* behavior and cannot be characterized using the 3ω method. Besides, when using the 3ω method, the temperature coefficient of the resistance also needs to be known,[4] which for most materials needs to be measured separately. For the microfabricated suspended device method, the tiny sample is placed between two membranes/islands. The heat transfer along the sample and the temperature difference between the membranes/islands are evaluated/characterized to determine the thermal conductivity of the sample. For samples with low thermal conductivity, the heat transfer between the two membranes/islands could become less accurate to evaluate. In addition, undesired heat conduction/radiation from the membranes could affect the final measurement result. The OHETS technique, developed by Hou *et al.*,[8,9] utilizes a periodically modulated laser beam to irradiate the sample to induce a periodical change in its electrical resistance. Meanwhile, a small dc is fed to the sample to probe its temperature variation. This technique can be used to measure the thermophysical properties of conductive, nonconductive, and semiconductive one-dimensional micro/nanoscale structures. The OHETS technique itself, like the 3ω method, requires relatively long measurement time (several hours) and suffers from low signal.

In this paper, a transient electrothermal (TET) technique is developed to overcome the drawback of the 3ω and OHETS techniques. Transient electrical heating and thermal sensing are used in the measurement. This technique can be applied to metallic, nonconductive, and semiconductive microscale wires. Compared with the 3ω and OHETS techniques, the technique developed in this work features much stronger signal level (hundreds to thousands of times higher) and much reduced measurement time (less than one second). To test this technique, thermal diffusivity measurement of platinum (Pt) wire specimens is conducted. By applying this technique, the thermal diffusivity of single-wall carbon nanotube (SWCNT) bundles and polyester fibers are also measured. In Sec. II, the experimental principle and physical model development are presented. The experimental details and results are discussed in Sec. III.

[a)]Author to whom correspondence should be addressed; FAX: (402) 472-1465; electronic mail: xwang3@unl.edu

 © 2007 American Institute of Physics

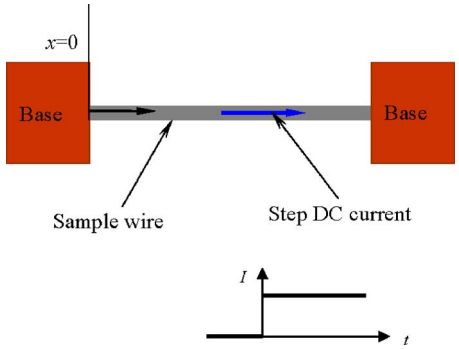

FIG. 1. (Color online) Schematic of the experimental principle and the step current for the TET technique.

II. EXPERIMENTAL PRINCIPLES AND PHYSICAL MODE DEVOLOPMENT

A. Experimental principles

In the TET technique, the to-be-measured wire is suspended between two copper electrodes as shown in Fig. 1. At the beginning of the experiment, a dc (shown in Fig. 1) is fed through the wire to introduce electrical heating. The temperature increase history of the wire is tightly related to the heat transfer along it. For example, with the same length, if the wire has small thermal diffusivity, it will take a long time to reach its steady state temperature. The temperature change of the wire will lead to its resistance change, which can change the voltage over the wire. In the experiment, the temperature change of the wire will be monitored by measuring the voltage variation over it. Once the temperature evolution is obtained, the thermal diffusivity of the wire can be obtained by fitting the temperature change curve against time. If the to-be-measured wire is nonconductive, a thin film of metal, like Au used in this work, should be coated on the surface of the wire for the purpose of making it electrically conductive. In the experiment, the length of the wire should be much larger than its diameter, which will simplify the physical mode to one dimensional.

B. Physical mode development

Figure 1 shows that the heat transfer problem is one dimensional along the wire (x direction). In the experiment, the electrical heating power has the form of $Q(t)=H(t)q_0$, where $H(t)$ is the Heaviside function and q_0 is the electrical heating power per unit volume. Here q_0 is assumed to be constant. In real situations the heating power changes a little bit and will be discussed in the following section. The initial condition of the problem is $T(x,t=0)=T_0$, where T_0 is the room temperature. Since the copper electrodes used in the experiments are much larger than the sample dimension, the temperature of the electrodes can be assumed constant even if a small current is flowing through them. Thus, the boundary conditions are reasonably described as $T(x=0,t)=T(x=L,t)=T_0$. For the heat transfer in the wire along the x direction at time $t\geqslant 0$ without considering radiation (detailed in work by Hou *et al.*[10]), the governing equation is

$$\frac{\partial(\rho c_p T)}{\partial t} = k\frac{\partial^2 T}{\partial x^2} + q_0, \tag{1}$$

where ρ, c_p, and k are the density, specific heat, and thermal conductivity of the wire, respectively. To make the solution development more feasible, we assume these properties are constant and independent of temperature. The solution to the partial differential equation can be obtained by integral of Green's function,[11]

$$G_{X11}(x,t|x',\tau) = \frac{2}{L}\sum_{m=1}^{\infty} \exp[-m^2\pi^2\alpha(t-\tau)/L^2] \times \sin\left(m\pi\frac{x}{L}\right)\sin\left(m\pi\frac{x'}{L}\right). \tag{2}$$

The temperature distribution along the wire is expressed as $T(x,t)=T_0+\frac{\alpha}{k}\int_{\tau=0}^{t}\int_{x'=0}^{L} q_0 G_{X11}dx'd\tau$. The average temperature of the wire $T(t)$ can be integrated and calculated as below:

$$T(t) = \frac{1}{L}\int_{x=0}^{L} T(x,t)dx = T_0 + \frac{8q_0L^2}{k\pi^4}\sum_{m=1}^{\infty}\frac{1-\exp[-(2m-1)^2\pi^2\alpha t/L^2]}{(2m-1)^4}. \tag{3}$$

When time goes to infinity ($t\rightarrow\infty$), the temperature distribution along the wire will reach the steady state. The final steady state average temperature of the wire is

$$T(t\rightarrow\infty) = T_0 + \frac{q_0L^2}{12k}. \tag{4}$$

The normalized temperature increase, which is defined as $T^*(t)=[T(t)-T_0]/[T(t\rightarrow\infty)-T_0]$, can be written as

$$T^* = \frac{96}{\pi^4}\sum_{m=1}^{\infty}\frac{1-\exp[-(2m-1)^2\pi^2\alpha t/L^2]}{(2m-1)^4}. \tag{5}$$

If normalizing time (x axis) to the Fourier number as $Fo=\alpha t/L^2$, it can be concluded from Eq. (5) that, to any kinds of material with any length, the normalized temperature increase follows the same shape with respect to Fo.

C. Methods for data analysis to determine the thermal diffusivity

After the temperature evolution $T\sim t$ of the wire is obtained by the experiment, different methods can be used to obtain the thermal diffusivity of the wire from this temperature history. Figure 2 shows a typical normalized temperature increase as an example to discuss the methods for data analysis. In this work, three methods are specifically designed and discussed.

1. Linear fitting at the initial stage of electrical heating

At the very beginning of electrical heating, $0<t<\Delta t$ (where Δt is very small), the temperature gradient along the wire is extremely small. The heat transferred to the two ends during this period ($0\rightarrow\Delta t$) can be neglected. Therefore, the

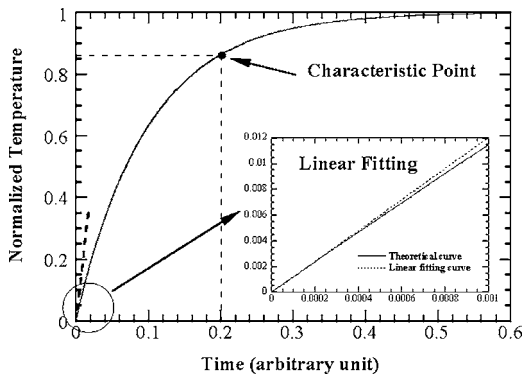

FIG. 2. Normalized theoretical curve and the corresponding data analysis methods.

temperature change with time can be described as $\Delta T = q_0/\rho c_p \Delta t$. The corresponding normalized temperature increase is $T^* = 12\alpha/L^2 \Delta t$. It is clear that the slope of the normalized temperature increase curve is $12\alpha/L^2$. Once the normalized temperature increase is obtained experimentally, linear fitting can be conducted for the initial data points to obtain the slope. Then with knowledge of the wire length, its thermal diffusivity can be readily determined.

Using the numerical method, we can get the idea about how large Δt can be used to fit the thermal diffusivity. We plot out (shown in Fig. 2) the normalized temperature increase curve and the linear fitting result from zero until the difference between them is larger than 5%. When the difference reaches 5%, the corresponding Fourier number is 0.001. This provides, together with the length, the guidance on within what time the linear fitting method can be used. From Fig. 2, it is estimated that the experimental data points up to 0.2% of the time it takes to reach steady state can be used for the linear fitting.

2. Characteristic point method

It is seen from Eq. (5) that the normalized temperature is only a function of $\alpha t/L^2$. Therefore, one characteristic point of the $T \sim t$ curve can be used to determine the thermal diffusivity directly. The best characteristic point should have the properties that both the y axis (normalized temperature) and x axis (time) have large changes when the thermal diffusivity makes a small change of $\Delta\alpha$. That is to say we need the product $\Delta T^* \Delta t$ to have the maximum value when the thermal diffusivity changes by $\Delta\alpha$, where $\Delta T^* = \partial T^*/\partial\alpha \cdot \Delta\alpha$ and $\Delta t = \partial t/\partial\alpha \cdot \Delta\alpha$. In order to get the maximum value at the change of $\Delta\alpha$, the term $\partial T^*/\partial\alpha \cdot \partial t/\partial\alpha$ should reach its maximum value. It is not difficult to find that $\partial T^*/\partial\alpha \cdot \partial t/\partial\alpha = \partial T^*/\partial Fo \cdot Fo^2/\alpha^3$.

Using Eq. (5), it is relatively easy to find that we can get the best characteristic point when T^* is 0.8665. The corresponding Fourier number is 0.2026, which is shown in Fig. 2. In the characteristic point method, like the laser flash technique,[12] once the characteristic time (Δt_c) is identified from the $T^* \sim t$ curve when the normalized temperature rise reaches 0.8665, the thermal diffusivity of the sample can be calculated as $\alpha = 0.2026 L^2/\Delta t_c$.

It needs to be mentioned that when using the characteristic point method, a small set of points around the characteristic point are chosen to conduct linear fitting to determine the characteristic point. This will substantially reduce the experimental uncertainty induced by data fluctuation.

3. Least square fitting method

The two fitting methods discussed above only use some local experimental data. Another technique is to employ global fitting of the experimental data to find the thermal diffusivity. In this method, the normalized temperature increase is calculated using Eq. (5) by using different trial values of the thermal diffusivity. The trial value giving the best fit (least square) of the experimental data is taken as the sample's thermal diffusivity.

D. Effect of nonconstant electrical heating

In Eq. (1) as discussed above, the electrical heating is assumed constant through all the transient process. In practice, the temperature increase of the wire will change its electrical resistance. The heating power therefore will be changed as well. This undesired heating power change can distort the voltage rise shape, leading to appreciable uncertainty. In this work, great efforts are exercised to reduce the heating power variation during the experiment.

If a constant current is fed through the sample, a resistor (R_{res}) with the same resistance as the sample needs to be connected with the sample in parallel. If the sample's resistance increases, the current through it will decrease, leading to a much more stable heating power over the sample. For instance, if the sample has a resistance of R_0 at room temperature and the current though the parallel connection is I, the heating power through the wire will be $I^2 R_0/4$ at the very beginning. Suppose the resistance of the sample changes from R_0 to $R_0(1+\beta)$ (here β is a fraction of resistance change $\Delta R/R_0$) the electrical heating power will change to $I^2 R_0(1+\beta)/(2+\beta)^2$. It can be observed that even if the resistance changes by 50%, the heating power only decreases by about 4%.

Similarly, if a constant voltage is supplied to the sample, a resistor with the same resistance as the wire needs to be serially connected with the wire. In the experiment, if the resistance of the wire increases, the voltage applied over it will increase as well, leading to a stable heating power over the wire. It is estimated that even if the resistance of the wire increases by 20%, the heating power over the wire will decrease less than 1%. It is conclusive that the nonconstant heating power problem can be readily solved with the above circuit designs.

III. EXPERIMENTAL DETAILS AND RESULTS

A. Experimental setup

Figure 3(a) shows the diagram of the experimental setup. The Wheatstone bridge is used to distinguish and measure the small voltage change over the wire. The other resistors in the circuit are rheostats. A set of batteries connected in series is used as the power source. This is because, in the experi-

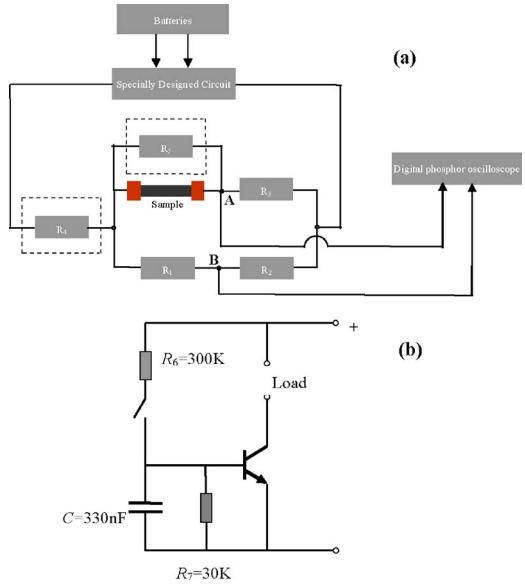

FIG. 3. (Color online) Schematic of the experiment setup and the specially designed circuit.

ments, batteries are much better than a dc power supply in terms of providing low noise voltage/current. In the experiment, the current/voltage applied to the sample needs to have a sharp rising curve as shown in Fig. 1. Otherwise, the long rising time of the heating power will introduce large uncertainty to the final temperature evolution. A specially designed fast switch circuit is used in the experiment to close the circuit [shown in Fig. 3(b)]. In addition, this circuit can eliminate the voltage oscillation (~2 ms) induced by a normal mechanical switch, leading to more stable heating in the beginning. A high speed digital oscilloscope TDS7054 is used to record the voltage evolution. All the elements in the experiment are connected with shielded cables to suppress noise from the environment. In order to minimize the influence of air convection, the wire is housed in a vacuum chamber where the pressure is maintained below 1×10^{-3} Torr.

The voltage evolution recorded by the oscilloscope is directly related to the average temperature change of the wire as

$$U_{AB} = \frac{R_2R_0U\eta}{(R_1+R_2)[R(t)+R_3]}\frac{8q_0L^2}{k\pi^4} \times\sum_{m=1}^{\infty}\frac{1-\exp[-(2m-1)^2\pi^2\alpha t/L^2]}{(2m-1)^4}, \quad (6)$$

where U_{AB} is the voltage across the bridge recorded by the oscilloscope, U is the constant voltage applied to the Wheatstone bridge, and η is the temperature coefficient of the resistance for the sample, which is assumed constant for the small temperature change. In Eq. (6), it can be observed that the term ahead of the infinite sum $8R_2R_0U\eta q_0L^2/(R_1+R_2)\times[R_3+R(t)]k\pi^4$ almost maintains constant for the small resistance change $R(t)$ during the experiment. It is clear that the measured voltage curve represents the temperature change of the sample.

TABLE I. Properties of the Pt wire (300 K) (Ref. 13) used in the calculation.

	Pt wire
Density (kg/m^3)	2.145×10^4
Specific heat (J/kg K)	133
Thermal conductivity (W/m K)	71.6
Electrical resistivity (Ω m)[a]	0.1086×10^{-6}
Temperature coefficient of resistance η (K^{-1})[a]	0.003927

[a]These properties are from Ref. 14. At 300 K, the electrical resistivity of Pt is $0.106\times10^{-6}/[1+(293.15-273.15)\times0.003\,927]\times[1+(300-273.15)\times0.003\,927]=0.1086\times10^{-6}$ Ω m.

B. System calibration

In order to verify this thermal characterization technique and the theoretical model developed in Sec. II, microscale Pt wires (properties shown in Table I) are measured. Three Pt wires with different lengths are measured. The experimental conditions are listed in Table II.

All the three data analysis methods are used to determine the thermal diffusivity as shown in Table II. By using the least square fitting method (method 3), the thermal diffusivity of the three Pt wires is fitted to be 2.53×10^{-5}, 2.54×10^{-5}, and 2.78×10^{-5} m^2 s^{-1}, respectively, close to the literature value of 2.51×10^{-5} m^2 s^{-1} (at 300 K). The characteristic point method (method 2) also gives close thermal diffusivity 2.47×10^{-5}, 2.41×10^{-5}, and 2.67×10^{-5} m^2 s^{-1} for the three samples, respectively. However, the linear fitting method (method 1) at the initial stage of electrical heating always has large deviation in comparison with the literature value. This is because at the initial stage of electrical heating, very limited data points are available. In order to have better fitting accuracy, more data points are used. These data points are beyond the time for $Fo=0.001$. Therefore, heat conduction becomes more important, making the fitted thermal diffusivity smaller than the real value of the sample. Figure 4 shows the fitting results using the three methods for

TABLE II. Details of experimental conditions for the Pt wires characterized in the experiment (using all the three data analysis methods).

	Pt wire 1	Pt wire 2	Pt wire 3
Length (mm)	5.08	5.07	5.78
Diameter (μm)	25.4	25.4	25.4
Resistance of sample (Ω)	1.274	1.244	1.499
dc current (mA)	78.06	85.02	93.51
Thermal diffusivity (10^{-5} m^2 s^{-1}) by method 1	1.89	2.01	2.41
Thermal diffusivity (10^{-5} m^2 s^{-1}) by method 2	2.47	2.41	2.67
Thermal diffusivity (10^{-5} m^2 s^{-1}) by method 3	2.53	2.55	2.78

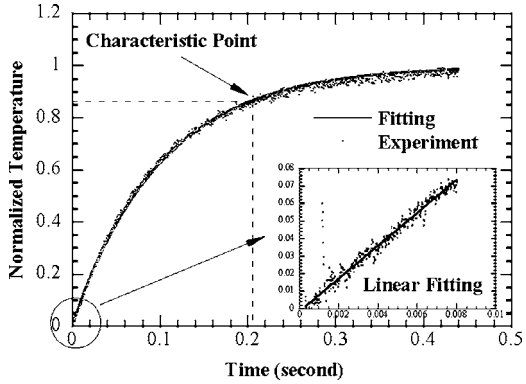

FIG. 4. The normalized temperature vs the theoretical fitting for the Pt wire (sample 2) using all the three data analysis methods.

Pt wire 2. Sound agreement is observed between the fitting results and the experimental data for the global least square fitting method. For this wire, the time taken to reach the steady state is about 0.4 s. As we discussed above, the time within which the data points can be used for initial linear fitting is 0.0008 s. However, the data points within this time are very limited. Therefore data points up to 0.008 s are used for linear fitting, leading to much reduced thermal diffusivity. For these reasons only the characteristic point and global fitting methods are used for thermal characterization of other samples.

Taking the data of Pt wire 1 as an example to estimate the temperature rise of the sample, the electrical heating power per unit volume along the wire is 3.02×10^{9} W m^{-3} calculated from $4I^2R/\pi D^2L$. Using Eq. (4), it can be obtained that the average temperature increase is about 90.6 °C. For the TET technique developed in this work, a linear *R-T* relation is needed. For Pt, the temperature coefficient of resistance is 0.003 927 within the temperature range of 0–100 °C.[14] indicating a linear *R-T* relation. Usually, a temperature increase of tens of degrees is required to obtain sound signals for the TET technique. For this level of temperature increase, the *R-T* relation for most metals can be treated linear with sound accuracy. The nonlinear feature in the *R-T* relation will induce some second-order negligible uncertainty in final data processing.

C. SWCNT bundles

In this section, SWCNT bundles are measured by using the established TET technique and the developed solution. Centimeters-long ropes of well-aligned SWCNT bundles were synthesized using a H_2/Ar arc discharge method. The synthesis process is detailed in work by Liu *et al.*[15] The structure and dimension of these SWCNT bundles were studied in our recent work using Raman scattering and scanning electron microscopy (SEM).[10] The SEM observation shows that there are threads from a few to tens of nanometers inside the SWCNT bundle and the threads do not follow the axial direction of the bundle. Besides, various size pores exist in the bundle.[10] The typical thickness/diameter of the SWCNT bundle is measured to be around 60 μm. Raman scattering study of the sample confirms existence of SWCNTs and concludes their primary diameter is 1.75 nm.

TABLE III. Details of experimental conditions and results for the SWCNT bundle.

	SWCNT bundles
Length (mm)	1.31
Resistance of sample (Ω)	93.3
dc current (mA)	8.039
α (10^{-5} m^2 s^{-1}) by method 2 for data 1	2.72
α (10^{-5} m^2 s^{-1}) by method 3 for data 1	2.72
α (10^{-5} m^2 s^{-1}) by method 2 for data 2	2.72
α (10^{-5} m^2 s^{-1}) by method 3 for data 2	2.74

When measuring SWCNT bundles, the TET technique is especially effective for the reason that the resistance of the SWCNT bundles has a long-time drift. The short measurement time of the TET technique eliminates the effect of this long-time resistance drift. For other steady state measurement techniques usually taking several hours, it will introduce appreciable uncertainties to the experiment because of the resistance change. In the experiment, the SWCNT bundles are connected between two copper electrodes using silver paste. Table III shows the length, resistance, and other parameters of the SWCNT bundle measured in the experiment. When conducting experiments, it is observed that the temperature coefficient of resistance for the SWCNT bundles is negative. The thickness/diameter of the SWCNT bundle is measured to be around 65 μm. Under this condition, radiation heat loss from the bundle surface can be neglected compared with the heat conduction along the bundle. Lack of knowledge about the density and specific heat of the SWCNT bundle makes it difficult to measure their thermal conductivity directly. Instead, the thermal diffusivity of the sample can be characterized based on the $T\sim t$ curve.

The experiment is conducted several times to measure the thermal diffusivity of the same SWCNT bundle. The characteristic point (method 2) and least square global data fitting (method 3) methods are used to determine the thermal diffusivity of the sample. The experimental conditions and two sets of result are shown in Table III. For the first set of data measured in the experiment, the thermal diffusivity is fitted to be 2.72×10^{-5} and 2.72×10^{-5} m^2/s using method 2 and 3, respectively. For the second set of data, the fitting results are 2.72×10^{-5} and 2.74×10^{-5} m^2/s, respectively. Figure 5 shows the characteristic point method and the least square fitting method for the first set of data. The average value of the thermal diffusivity of the above stated SWCNT bundle is 2.73×10^{-5} m^2/s. The result is consistent with that obtained using the OHETS technique.[9] The sample is measured several times to check the repeatability of the technique and about 1% deviation is obtained.

D. Polyester fibers

As discussed above, the reported transient technique can also be used for measuring nonconductive micro/nanoscale wires/fibers. In this section, microscale polyester fibers are measured. In the experiment, a thin Au film is coated on the surface of the fiber to make it possible to conduct transient electrical heating and thermal sensing. The SEM picture of

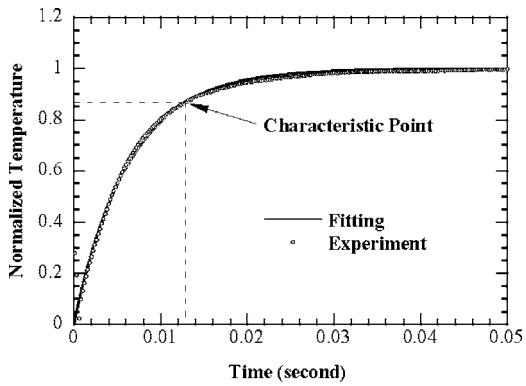

FIG. 5. The normalized temperature vs the theoretical fitting for the SWCNT bundle.

one of the measured fibers is shown in Fig. 6. It is observed that the fiber is around 10 μm thick. Since Au is an excellent conductor for heat transfer, the coated Au film will have some effect on the measured thermal diffusivity, especially for thin wires. The effect of the coated Au film can be ruled out using the concept of thermal conductance. The thermal conductance (G_f) of the Au film is defined as $G_f = A_f k_f / L$, where k_f and A_f are the thermal conductivity and the cross-sectional area of the thin film, respectively. It is known that k_f can be much smaller than the bulk material's value due to the unique structure and small thickness of the thin film coating. Here G_f is evaluated using the Wiedemann-Franz law, which relates the thermal conductivity (k) of the metal to its electrical conductivity (σ) as $L_{\text{Lorenz}} = k/(\sigma T)$. The Lorenz number for Au is weakly dependent on temperature: 2.35×10^{-8} W Ω K^{-2} at 0 °C and 2.40×10^{-8} W Ω K^{-2} at 100 °C.[16] Based on the formula above, the thermal conductance of the coated thin film can be calculated as $G_f = L_{\text{Lorenz}} T / R$.

In the experiment, the measured effective thermal diffusivity (α_e) is the combined effect of the wire and the Au thin film, which can be described as

$$\alpha_e = \frac{k(1-\chi) + k_f \chi}{\rho c_p (1-\chi) + \rho_f c_{p,f} \chi}, \tag{7}$$

where ρ_f and $c_{p,f}$ are the density and specific heat of the Au film. $\chi = A_f / A_e$ is the cross-sectional ratio of the Au film, where A_e and A_w are the cross-sectional area of coated and bare wires, respectively. Since $\chi \ll 1$, we can estimate that

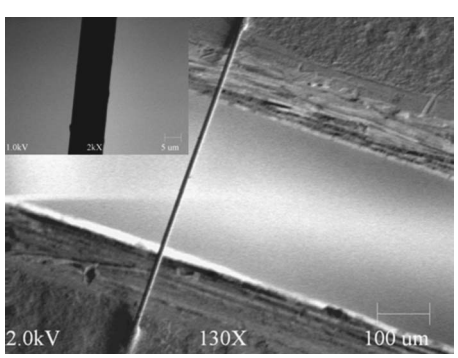

FIG. 6. SEM picture of coated polyester fiber (sample 2).

TABLE IV. Details of experimental conditions and results for the polyester fibers.

	Sample 1	Sample 2
Length (μm)	679.25	590.1
Diameter (μm)	10.33	10.46
Resistance of sample (kΩ)	2.95	319
dc current (μA)	431.5	11.76
α_e (10^{-7} m^2/s)	6.800	5.260
$k_f \beta / \rho c_p$ (10^{-7} m^2/s)	0.123	0.001
α (10^{-7} m^2/s)	6.677	5.259

$\rho c_p (1-\chi) \gg \rho_f c_{p,f} \chi$ and $(1-\chi) \approx 1$. Equation (7) can be simplified as

$$\alpha_e = \frac{k + k_f \chi}{\rho c_p} = \alpha + \frac{k_f \chi}{\rho c_p}. \tag{8}$$

Since $k_f \chi = (L_{\text{Lorenz}} T / R) L / A_w$, the real thermal diffusivity of the wire (α) can be calculated as

$$\alpha = \alpha_e - \frac{L_{\text{Lorenz}} T L}{R A_w \rho c_p}. \tag{9}$$

The density and specific heat[17] of polyester are $\rho = 1.368 \times 10^3$ kg m^{-3} and $c_p = 1.2 \times 10^3$ J kg^{-1} K^{-1}, respectively. In the TET experiment, the contact resistance at the ends of the sample could change the heating style of the sample and alter the value R used in Eq. (9). In order to reduce the contact resistance between the polyester fiber and copper electrodes, the fiber is coated first and then connected to the electrodes using silver paste. This will make the coating have sound contact with the silver paste, leading to a small contact resistance. Two samples of polyester fibers are coated for thermal diffusivity measurement, one with a bigger resistance and the other one with a smaller resistance. The experimental conditions are summarized in Table IV. It needs to be pointed out that the measured resistances inevitably consist of contact resistance and the coating resistance. In the experiment for Pt, it is estimated the silver paste leads to a contact resistance about 0.2 ~ 0.3 Ω. Since the measured polyester fibers have comparable thickness to that of the measured Pt wires, the contact resistance between the Au coating on the fiber and the silver paste is expected to be small compared with the resistance of the Au coating that is in the order of a few to hundreds of kilo-ohms.

Using global data fitting, the real thermal diffusivity of the fiber is measured to be 6.68×10^{-7} m^2/s for sample 1 and 5.26×10^{-7} m^2/s for sample 2. Figure 7 shows the fitting curve for sample 2 using the global data fitting and characteristic point methods. Experiments are conducted for a number of rounds and it is found that a repeatability better than 10% can be achieved. It is observed that for a coated wire with a smaller resistance, the measured thermal diffusivity is larger. This is because the smaller resistance means a thicker coating on the wire. Therefore, the heat transfer along the wire is partially controlled by the Au film coating. The assumption used to derive Eq. (9) becomes less accurate. Another possible reason for the larger thermal diffusivity of the smaller resistance sample is that when the Au coating is

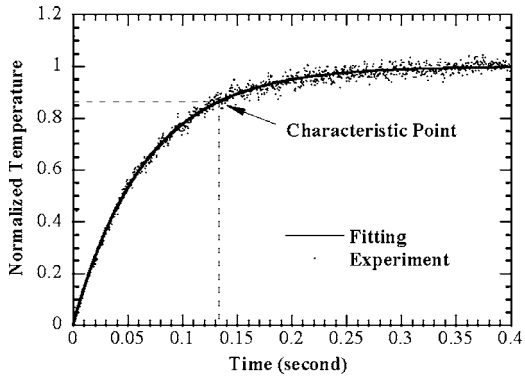

FIG. 7. The normalized temperature vs the theoretical fitting for polyester fiber (sample 2).

thick, its electrical resistance is small. Under this situation, the contact resistance plays a more important role in affecting the resistance R used in Eq. (9) and makes it larger. This will lead to a smaller thermal diffusivity subtraction in Eq. (9), making the final thermal diffusivity larger. Our extensive experiments prove that in order to obtain high accuracy in measuring the thermal diffusivity of nonconductive wires, the Au coating on the wire needs to be as thin as possible, meaning a large electrical resistance is preferred. In this work, the electrical contact between the wire and electrode is enhanced using silver paste. For nanometer wires, a much improved technique is needed. Focused ion beam deposition of Pt provides a better way to enhance the electrical contact between the nanowire and electrode.

IV. CONCLUSION

In this paper, a fast transient technique is developed to characterize the thermophysical properties of micro/nanoscale wires/tubes. Transient electrical heating and thermal sensing are employed in the technique to have a significantly improved signal level. Three methods are developed for data analysis to obtain the thermal diffusivity of the sample. Employing this technique, the thermal diffusivity of Pt wires is measured. The measurement results agree well with the reference value. Our uncertainty analysis shows that the experiment has an uncertainty better than 10%. We have measured the thermal diffusivity of SWCNT bundles and the average value was 2.73×10^{-5} m^2/s, which is much smaller than that of graphite in the layer direction. Finally, polyester fibers are measured to demonstrate the capability of the technique for thermal characterization of nonconductive wires/tubes. The measured thermal diffusivity after the amendment is 5.26×10^{-7} m^2/s.

ACKNOWLEDGMENTS

This work was supported by National Science Foundation (CMS: 0457471), Nebraska Research Initiative, Air Force Office for Scientific Research, and MURI from ONR. SWCNT bundles were provided by Chang Liu and Huiming Cheng from Shenyang National Laboratory for Materials Science, Chinese Academy of Sciences. The authors really appreciate this strong support.

[1]L. Lu, W. Yi, and D. L. Zhang, Rev. Sci. Instrum. **72**, 2996 (2001).
[2]X. Wang, P. Vellelacheruvu, J. Hou, J. Guo, C. Liu, and H. Cheng, The 9th AIAA/ASME Joint Thermophysics and Heat Transfer Conference, San Francisco, California (American Institute of Aeronautics and Astronautics, Reston, VA, 2006), Paper No. 3122.
[3]T. Y. Choi, D. Poulikakos, J. Tharian, and U. Sennhauser, Appl. Phys. Lett. **87**, 013108 (2005).
[4]T. Y. Choi, D. Poulikakos, J. Tharian, and U. Sennhauser, Nano Lett. **6**, 1589 (2006).
[5]P. Kim, L. Shi, A. Majumdar, and P. L. McEuen, Phys. Rev. Lett. **87**, 215502 (2001).
[6]L. Shi, D. Li, C. Yu, W. Jang, D. Kim, Z. Yao, P. Kim, and A. Majumdar, J. Heat Transfer **125**, 881 (2003).
[7]D. Li, Y. Wu, P. Kim, L. Shi, P. Yang, and A. Majumdar, Appl. Phys. Lett. **83**, 2934 (2003).
[8]J. Hou, X. Wang, and J. Guo, J. Phys. D **39**, 3362 (2006).
[9]J. Hou, X. Wang, C. Liu, and H. Cheng, Appl. Phys. Lett. **88**, 181910 (2006).
[10]J. Hou, X. Wang, P. Vellelacheruvu, J. Guo, C. Liu, and H. Cheng, J. Appl. Phys. **100**, 124314 (2006).
[11]J. V. Beck, K. D. Cole, A. Haji-Sheikh, and B. Litkouhi, in *Heat Conduction Using Green's Functions* (Hemisphere, New York, 1992), p. 482.
[12]W. J. Parker, R. J. Jenkins, C. P. Butler, and G. L. Abbott, J. Appl. Phys. **32**, 1679 (1961).
[13]F. Incropera and D. Dewitt, in *Fundamentals of Heat and Mass Transfer*, 5th ed. (Wiley, New York, 2002).
[14]R. Weast, *Handbook of Chemistry and Physics*, 64th ed. (CRC, Boca Raton, Florida, 1983), p. F-125.
[15]C. Liu, H. M. Cheng, H. T. Cong, F. Li, G. Su, B. L. Zhou, and M. S. Dresselhaus, Adv. Mater. (Weinheim, Ger.) **12**, 1190 (2000).
[16]C. Kittel, in *Introduction to Solid State Physics*, 5th ed. (Wiley, New York, 1976), p. 178.
[17]L. Olenka *et al.*, J. Phys. D **34**, 2248 (2001).